J|A|C|S ARTICLES

Published on Web 01/22/2010

Strain-Induced Cleavage of Carbon−Carbon Bonds: Bridge Rupture Reactions of Group 8 Dicarba[2]metallocenophanes

David E. Herbert, Joe B. Gilroy, Anne Staubitz, Mairi F. Haddow, Jeremy N. Harvey,* and Ian Manners*

School of Chemistry, University of Bristol, Cantock's Close, Bristol, BS8 1TS, United Kingdom

Received October 13, 2009; E-mail: Jeremy.Harvey@bristol.ac.uk; Ian.Manners@bristol.ac.uk

Abstract: Thermal treatment of dicarba[2]ferrocenophanes [Fe(η^5-C_5H_4)$_2$(CMe_2)$_2$] (**1**), *rac*-[Fe(η^5-C_5H_4)$_2$(CH*i*Pr)$_2$] (*rac*-**5**), and *meso*-[Fe(η^5-C_5H_4)$_2$(CH*t*Bu)$_2$] (*meso*-**7**) at 240−300 °C in the melt led to cleavage of the carbon−carbon bond in the bridge. Compounds **1** and *rac*-**5** underwent intramolecular abstraction of H• and yielded ring-opened, vinyl-substituted 1,1'-metallocenes, while *meso*-**7** thermally converted to the more thermodynamically stable *rac* isomer. The corresponding dicarba[2]ruthenocenophanes [Ru(η^5-C_5H_4)$_2$(CMe_2)$_2$] (**10**), *rac*-[Ru(η^5-C_5H_4)$_2$(CH*i*Pr)$_2$] (*rac*-**12**), and *meso*-[Ru(η^5-C_5H_4)$_2$(CH*t*Bu)$_2$] (*meso*-**15**) underwent analogous thermal carbon−carbon bond cleavage but more readily, consistent with a higher degree of ring strain. In the case of **7** and **15**, the stability of the *rac* isomers relative to the respective *meso* isomers was confirmed by DFT studies, despite the former species exhibiting slightly higher tilt angles (α/deg) between the two cyclopentadienyl (Cp) rings. Theoretical investigations were used to explore the mechanism of carbon−carbon bond cleavage in dicarba[2]metallocenophanes, confirming the validity of the proposed homolytic bond cleavage mechanism. In addition, the potential role of bis-fulvene metal(0) and 'tuck-in' complexes in the bond-cleavage mechanism was assessed. This study also provides insight into the mechanism of the thermal ring-opening polymerization of $-CH_2CH_2-$ bridged dicarba[2]metallocenophanes and, for the first time, supports a homolytic carbon−carbon bond cleavage pathway.

1. Introduction

The activation of carbon−carbon (C−C) σ bonds has long been an area of great interest to synthetic chemists.[1] More recently, C−C bond cleavage has been observed during phosphinothricin biosynthesis[2] and in surface-adsorbed macromolecules.[3] Despite the relatively higher bond enthalpies associated with C−H bonds, their activation is much more frequently observed than in the case of C−C bonds. However, significant progress has been made toward the insertion of metal centers into the latter, one of the first steps required in potential catalytic C−C bond activation.[4] To facilitate selective C−C bond cleavage, a number of driving forces have been employed. These include the introduction of aromaticity into the C−C bond cleavage products,[5] the enforced close proximity of a C−C bond to a low valent transition metal fragment,[6] and the potential for the relief of ring strain in substrates such as biphenylene.[7]

Ansa metallocenes, or [*n*]metallocenophanes,[8] with short bridges ($n \leq 2$) and more than four d electrons contain significant molecular strain,[9] and the relief of this ring strain can be exploited in a number of ways, notably in the preparation of polymetallocenes through ring-opening polymerization (ROP).[10−12] For heteroatom-bridged [1]metallocenophanes, a large majority of the reported reactivity has been observed under ambient conditions at an exposed, polarized C_{ipso}−E bond (e.g., E = Si, P, Ge, Sn, Al, and Ga),[13] while selective metal−cyclopentadienyl (Cp) bond reactivity is a more recent development.[14,15] [2]Metallocenophanes (Figure 1) can show enhanced reactivity at the bridging E−E moiety, and many examples of oxidative addition of late-transition metal centers with subsequent insertion

(1) Crabtree, R. H. *Chem. Rev.* **1985**, *85*, 245–269.
(2) Cicchillo, R. M.; Zhang, H.; Blodgett, J. A. V.; Whitteck, J. T.; Li, G.; Nair, S. K.; van der Donk, W. A.; Metcalf, W. W. *Nature* **2009**, *459*, 871–875.
(3) Sheiko, S. S.; Sun, F. C.; Randall, A.; Shirvanyants, D.; Rubinstein, M.; Lee, H.-I.; Matyjaszewski, K. *Nature* **2006**, *440*, 191–194.
(4) (a) Rybtchinski, B.; Milstein, D. *Angew. Chem., Int. Ed.* **1999**, *38*, 871–883. (b) Jun, C.-H. *Chem. Soc. Rev.* **2004**, *33*, 610–618. (c) Park, Y. J.; Park, J.-W.; Jun, C.-H. *Acc. Chem. Res.* **2008**, *41*, 222–234.
(5) Halcrow, M. A.; Urbanos, F.; Chaudret, B. *Organometallics* **1993**, *12*, 955–957.
(6) van der Boom, M. E.; Milstein, D. *Chem. Rev.* **2003**, *103*, 1759–1792.
(7) Perthuisot, C.; Edelbach, B. L.; Zubris, D. L.; Simhai, N.; Iverson, C. N.; Muller, C.; Satoh, T.; Jones, W. D. *J. Mol. Catal. A: Chem.* **2002**, *189*, 157–168.
(8) For recent highlights in the area of metallocenophanes and related compounds, see: (a) Herdtweck, E.; Jäkle, F.; Wagner, M. *Organometallics* **1997**, *16*, 4737–4745. (b) Sinnema, P.-J.; Shapiro, P. J.; Foo, D. M. J.; Twamley, B. *J. Am. Chem. Soc.* **2002**, *124*, 10996–10997. (c) Sharma, H. K.; Cervantes-Lee, F.; Pannell, K. H. *J. Am. Chem. Soc.* **2004**, *126*, 1326–1327. (d) Chadha, P.; Dutton, J. L.; Sgro, M. J.; Ragogna, P. J. *Organometallics* **2007**, *26*, 6063–6065. (e) Lund, C. L.; Schachner, J. A.; Quail, J. W.; Müller, J. *J. Am. Chem. Soc.* **2007**, *129*, 9313–9320. (f) Whittell, G. R.; Partridge, B. M.; Presly, O. C.; Adams, C. J.; Manners, I. *Angew. Chem., Int. Ed.* **2008**, *47*, 4354–4357. (g) Braunschweig, H.; Breher, F.; Kaupp, M.; Gross, M.; Kupfer, T.; Nied, D.; Radacki, K.; Schinzel, S. *Organometallics* **2008**, *27*, 6427–6433. (h) Khramov, D. M.; Rosen, E. L.; Lynch, V. M.; Bielawski, C. W. *Angew. Chem., Int. Ed.* **2008**, *47*, 2267–2270. (i) Tamm, M. *Chem. Commun.* **2008**, 3089–3100.
(9) Green, J. C. *Chem. Soc. Rev.* **1998**, *27*, 263–272.
(10) Bellas, V.; Rehahn, M. *Angew. Chem., Int. Ed.* **2007**, *46*, 5082–5104.
(11) Herbert, D. E.; Mayer, U. F. J.; Manners, I. *Angew. Chem., Int. Ed.* **2007**, *46*, 5060–5081.
(12) Whittell, G. R.; Manners, I. *Adv. Mater.* **2007**, *19*, 3439–3468.

 10.1021/ja9087049

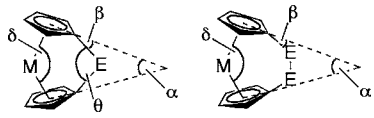

Figure 1. Bond angles in [1]- and [2]metallocenophanes.

of unsaturated organic substrates have been reported. For example, Pd(0) and Pt(0) catalysts have been used to insert alkynes into Si−Si[16] and Sn−Sn[17] bonds of [2]ferrocenophanes and [2]chromarenophanes,[18] and the homogeneous and heterogeneous diboration of alkynes and diazobenzene using B−B bonds of [2]metallarenophanes have been reported.[19] While thermal[20,21] and transition metal catalyzed[22] ROP of [1]ferrocenophanes has been shown to occur via activation of a C_{ipso}−E bond, the reactivity of group 14 E−E bonds in [2]metallocenophanes and related species suggests that Pd- and Pt-catalyzed ROP of tetramethyldigerma[2]ferrocenophane may also involve oxidative addition of a Ge−Ge bond.[23] Most recently, the remarkable intramolecular activation of the Si−Si bond in tetramethyldisila[2]molybdenocenophanedihydride and conversion to the corresponding bis(silyl) molybdenocene 'tuck-in' complex through photoinduced loss of hydrogen was described (Scheme 1).[24]

Comparison of the tilt angles of hydrocarbon-bridged [2]ferrocenophanes to sila[1]ferrocenophanes ($\alpha \approx 20°-23°$) suggests that the compounds have similar degrees of ring strain.[25,26]

Scheme 1. Cleavage of a Bridging Si−Si Bond in a [2]Molybdenocenophane[24]

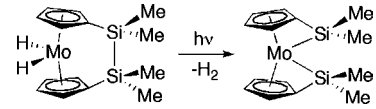

Scheme 2. Thermal ROP of Dicarba[2]metallocenophanes

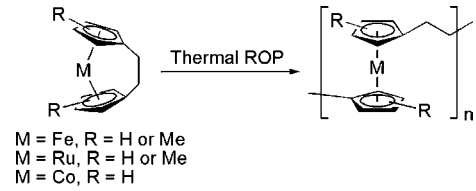

However, smaller β angles between the bridging element-C_{ipso} bond and the plane of the Cp ring (*ca.* 13° compared to 37°) and negligible polarization of this bond contribute to the lower reactivity of C_{ipso}−C_{bridge} bonds in dicarba[2]ferrocenophanes compared to C_{ipso}−Si_{bridge} bonds in sila[1]ferrocenophanes. Despite these considerations, hydrocarbon-bridged [2]metallocenophanes will undergo thermal ROP to give poly(metallocenylethylenes), although the mechanism of ring-opening remains unclear (Scheme 2).[25−27] Herein we report the cleavage of bridging C−C bonds of group 8 dicarba[2]metallocenophanes in the melt at elevated temperatures and detailed studies of this novel reactivity to gain insight into the mechanism of thermal ROP observed in related derivatives.

2. Results and Discussion

2.1. Thermal Chemistry of Dicarba[2]ferrocenophanes 1, 5, and 7. A sample of red crystals of 1,1,1',1'-tetramethylethylenyl[2]ferrocenophane **1** (melting point = 138 °C[28]) was sealed under vacuum in a glass tube and heated to 240 °C for 1.5 h. In typical thermal ROP experiments for polymerizable strained metallocenophanes, the solid samples melt and then become immobile as the polymerization proceeds.[29] In this case, the crystalline material melted to form a dark-red free-flowing liquid, which only partially resolidified upon cooling below 160 °C. The tube was then cooled to room temperature, and the contents were examined without further purification by ^{1}H NMR spectroscopy in C_6D_6. This analysis revealed a 39% conversion of the starting material to a single product with signals suggesting the presence of an *i*Pr group (septet, δ = 2.50 ppm; doublet, δ = 1.12 ppm, $^3J_{HH}$ = 6.85 Hz), olefinic protons (multiplets, δ = 5.21 and 4.89 ppm), and four distinct magnetic environments for the Cp protons (*pseudo*-triplets, δ = 4.25, 4.05, 3.91, 3.88 ppm). Following flash chromatography, the product was isolated as an orange oil in 18% yield and was identified by 1D and 2D NMR spectroscopy, mass spectrometry, and elemental analysis as the ring-opened, disubstituted metallocene **2** (Scheme 3). Longer reaction times (>16 h) did not

(13) (a) Seyferth, D.; Withers, H. P. *J. Organomet. Chem.* **1980**, *185*, C1–5. (b) Sheridan, J. B.; Lough, A. J.; Manners, I. *Organometallics* **1996**, *15*, 2195–2197. (c) Castruita, M.; Cervantes-Lee, F.; Mahmoud, J. S.; Zhang, Y.; Pannell, K. H. *J. Organomet. Chem.* **2001**, *637−639*, 664–668. (d) Mizuta, T.; Onishi, M.; Nakazono, T.; Nakazawa, H.; Miyoshi, K. *Organometallics* **2002**, *21*, 717–726. (e) Baumgartner, T.; Jäkle, F.; Rulkens, R.; Zech, G.; Lough, A. J.; Manners, I. *J. Am. Chem. Soc.* **2002**, *124*, 10062–10070. (f) Bourke, S. C.; MacLachlan, M. J.; Lough, A. J.; Manners, I. *Chem.−Eur. J.* **2005**, *11*, 1989–2000. (g) Schachner, J. A.; Tockner, S.; Lund, C. L.; Quail, J. W.; Rehahn, M.; Müller, J. *Organometallics* **2007**, *26*, 4658–4662. (h) Gómez-Elipe, P.; Macdonald, P. M.; Manners, I. *Angew. Chem., Int. Ed. Engl.* **1997**, *36*, 762–764.
(14) (a) Berenbaum, A.; Braunschweig, H.; Dirk, R.; Englert, U.; Green, J. C.; Jäkle, F.; Lough, A. J.; Manners, I. *J. Am. Chem. Soc.* **2000**, *122*, 5765–5774. (b) Mizuta, T.; Imamura, Y.; Miyoshi, K. *J. Am. Chem. Soc.* **2003**, *125*, 2068–2069. (c) Imamura, Y.; Kubo, K.; Mizuta, T.; Miyoshi, K. *Organometallics* **2006**, *25*, 2301–2307. (d) Tanabe, M.; Vandermeulen, G. W. M.; Chan, W. Y.; Cyr, P. W.; Vanderark, L.; Rider, D. A.; Manners, I. *Nat. Mater.* **2006**, *5*, 467–470. (e) Ieong, N. S.; Chan, W. Y.; Lough, A. J.; Haddow, M. F.; Manners, I. *Chem.−Eur. J.* **2008**, *14*, 1253–1263.
(15) Herbert, D. E.; Tanabe, M.; Bourke, S. C.; Lough, A. J.; Manners, I. *J. Am. Chem. Soc.* **2008**, *130*, 4166–4176.
(16) Finckh, W.; Tang, B. Z.; Lough, A.; Manners, I. *Organometallics* **1992**, *11*, 2904–2911.
(17) Herberhold, M.; Steffl, U.; Wrackmeyer, B. *J. Organomet. Chem.* **1999**, *577*, 76–81.
(18) Braunschweig, H.; Kupfer, T. *Organometallics* **2007**, *26*, 4634–4638.
(19) (a) Braunschweig, H.; Lutz, M.; Radacki, K. *Angew. Chem., Int. Ed.* **2005**, *44*, 5647–5651. (b) Braunschweig, H.; Kupfer, T.; Lutz, M.; Radacki, K.; Seeler, F.; Sigritz, R. *Angew. Chem., Int. Ed.* **2006**, *45*, 8048–8051. (c) Braunschweig, H.; Kaupp, M.; Adams, C. J.; Kupfer, T.; Radacki, K.; Schinzel, S. *J. Am. Chem. Soc.* **2008**, *130*, 11376–11393.
(20) Pudelski, J. K.; Foucher, D. A.; Honeyman, C. H.; Lough, A. J.; Manners, I.; Barlow, S.; O'Hare, D. *Organometallics* **1995**, *14*, 2470–2479.
(21) Pudelski, J. K.; Manners, I. *J. Am. Chem. Soc.* **1995**, *117*, 7265–7266.
(22) Temple, K.; Jäkle, F.; Sheridan, J. B.; Manners, I. *J. Am. Chem. Soc.* **2001**, *123*, 1355–1364.
(23) Mochida, K.; Shibayama, N.; Goto, M. *Chem. Lett.* **1998**, 339–340.
(24) Braunschweig, H.; Gross, M.; Radacki, K.; Rothgaengel, C. *Angew. Chem., Int. Ed.* **2008**, *47*, 9979–9981.
(25) Mayer, U. F. J.; Gilroy, J. B.; O'Hare, D.; Manners, I. *J. Am. Chem. Soc.* **2009**, *131*, 10382–10383.
(26) (a) Nelson, J. M.; Lough, A. J.; Manners, I. *Angew. Chem., Int. Ed.* **1994**, *33*, 989–991. (b) Nelson, J. M.; Nguyen, P.; Petersen, R.; Rengel, H.; Macdonald, P. M.; Lough, A. J.; Manners, I.; Raju, N. P.; Greedan, J. E.; Barlow, S.; O'Hare, D. *Chem.−Eur. J.* **1997**, *3*, 573–584.
(27) Nelson, J. M.; Rengel, H.; Manners, I. *J. Am. Chem. Soc.* **1993**, *115*, 7035–7036.
(28) Lentzner, H. L.; Watts, W. E. *Tetrahedron* **1971**, *27*, 4343–4351.
(29) (a) Foucher, D. A.; Tang, B. Z.; Manners, I. *J. Am. Chem. Soc.* **1992**, *114*, 6246–6248. (b) Resendes, R.; Nelson, J. M.; Fischer, A.; Jäkle, F.; Bartole, A.; Lough, A. J.; Manners, I. *J. Am. Chem. Soc.* **2001**, *123*, 2116–2126.

Scheme 3. Thermal Carbon−Carbon Bond Cleavage in **1**

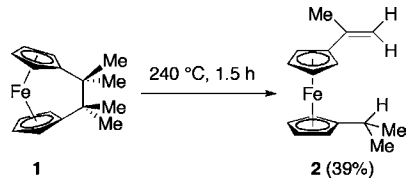

1 **2** (39%)

increase the yield of **2**, and in some cases further decomposition to unidentified products was observed.

Instead of undergoing ROP, the C−C bond bridging the two Cp rings of **1** ruptured and a hydrogen atom was abstracted from one methyl substituent to generate the *i*Pr and vinyl Cp-substituents of **2**. This is reminiscent of the reverse of the reductive coupling of 6,6-disubstituted fulvenes mediated by alkali, alkaline earth, and transition metals, used to form dicarba-bridged dicyclopentadienide salts (see Scheme 4, first 2 steps) which can then be employed in the synthesis of a range of [2]metallocenophanes, such as **1**.[30,31] As an example of this relevant reaction sequence, **1** and 1,1'-di-isopropylferrocene (**4**) were reported as the sole products upon warming a cocondensate of 6,6-dimethylfulvene and iron vapor to 0 °C.[32] A separate report of this synthesis described that direct reaction of 6,6-dimethylfulvene and iron vapor resulted in exclusive formation of **2**.[33] Both results may be explained by the formation of a diradical intermediate **3**, which may abstract H• from the surrounding environment to form **4**, convert to **1**, or engage in intramolecular H• abstraction (i.e., intramolecular disproportionation) to produce **2** (Scheme 5).[34] It is therefore likely that **3** forms as an intermediate in the thermal conversion of **1** to **2** (*vide infra*). Both radical−radical coupling and H• abstraction are classic decomposition pathways for reactive radicals. In the absence of stabilizing factors, classical radical intramolecular disproportionation reactions of reactive intermediates with diradical character (e.g., **3**) are to be expected.[35]

The di-isopropyl derivative, *rac*-1,1'-di-isopropylethylenyl[2]ferrocenophane *rac*-**5** (melting point = 177 °C), was prepared according to literature procedures[37] and was also found to undergo irreversible ring-opening with intramolecular H• abstraction when heated to 300 °C (Scheme 6). No conversion was observed, however, when a sealed, evacuated tube containing *rac*-**5** was heated to 225 °C for 16 h. After heating a sample to 300 °C for 16 h, the material remained dark red and free-flowing, and again, no immobilization (characteristic of ROP) was observed. The tube was opened and the products were found to be completely soluble in C_6D_6. ^{1}H NMR spectroscopy indicated 33% conversion from the strained starting material as calculated by a comparison of the integrals of signals assigned to *rac*-**5** and the ring-opened product **6**. Only one signal was assigned to an olefinic proton, while six protons were accounted for by methyl groups attached to the vinyl substituent of **6**, the formation of which may occur via abstraction of H• from one *i*Pr group, leaving the other intact. Compound **6** was isolated in 19% yield following separation from unreacted *rac*-**5** by column chromatography. Both ring-opened thermal products **2** and **6** eluted from silica columns before their respective strained [2]ferrocenophane precursor. Compounds **2** and **6** were isolated as orange oils which exhibit electronic absorption spectra in hexanes characteristic of substituted ferrocenes (**2**: $\lambda_{max} = 444$ nm, $\varepsilon = 225$ M^{-1} cm^{-1}; **6**: $\lambda_{max} = 447$ nm, $\varepsilon = 157$ M^{-1} cm^{-1}).

As the products resulting from the thermolysis of **1** and **5** appear to arise from H• abstraction in a diradical intermediate (e.g., **3**),[38] we decided to synthesize the *t*Bu-substituted derivative **7**. Compound **7**, like the $-CH_2CH_2-$ bridged analog which undergoes thermal ROP, lacks α-hydrogen substituents and also contains bulky *t*Bu groups, which may provide steric protection of the postulated diradical intermediate. The appropriate "fly-trap" dicyclopentadienide ligand was synthesized by the sodium-mediated reductive coupling of 6-*tert*-butylfulvene.[31] This was then converted to the Li^+ salt, and metathesis with $FeCl_2$ gave *meso*/*rac*-**7**. The crude material was sublimed at 40 °C and then recrystallized from THF/hexanes (1:4) to give *meso*/*rac*-**7** in 36% yield as a mixture of *meso*- and *rac*-**7** corresponding to different orientations of the *t*Bu groups. The mixture was characterized by ^{1}H and ^{13}C NMR spectroscopy, mass spectrometry, and elemental analysis. The ratio of isomers was determined using ^{1}H NMR spectroscopy to be 35:65 (*meso*:*rac*). Further reactivity was explored using this mixture.

In a similar fashion to the thermolysis of **1** and *rac*-**5**, a sealed tube containing a sample of *meso*- and *rac*-**7** (melting point of the mixture = 76−78 °C) was heated to 200 °C for 16 h. The contents of the tube again melted and did not immobilize. The tube was opened under an inert atmosphere, and the dark red residue was extracted with THF and sublimed at 50 °C to give pure *rac*-**7** (melting point = 125−126 °C) in 84% yield. As the isolated yield of *rac*-**7** exceeded the amount present in the starting material, heating the mixture of isomers *meso*/*rac*-**7** had cleanly converted *meso*-**7** to its *rac* counterpart (Scheme 7). In a repeat experiment, following heating at 150 °C and similar workup, *meso*/*rac*-**7** was reisolated in 82% yield with the ratio of isomers unchanged. This suggests that the temperature necessary to isomerize *meso*-**7** to *rac*-**7** lies between 150 and 200 °C. Following heating of a sample of the mixture *meso*/*rac*-**7** to 300 °C for 16 h, pure *rac*-**7** was reisolated in 93% yield. At this elevated temperature, a small amount of a dark black insoluble solid formed in the tube. The solid was readily attracted to a magnet, indicative of the presence of iron metal.

Single crystals of *meso*-**7** were isolated by recrystallization from a dilute hexanes solution of the mixture, from which the solid-state structure of the compound was determined by X-ray diffraction (Figure 2). The ^{1}H and ^{13}C NMR spectra of these crystals were collected to confirm the assignment of signals corresponding to *meso*-**7**. Single crystals of *rac*-**7** suitable for X-ray diffraction were grown by solvent evaporation of a hexanes solution of *rac*-**7**, and the structure of this isomer was also determined (Figure 3). In both structures, the Cp rings are planar and the relative orientation of the *t*Bu groups is evident.

(30) (a) Fischer, V. M.; Aebi, B.; Bonzli, P.; Grillo, S.; Neuenschwander, M. *Helv. Chim. Acta* **1999**, *82*, 1521–1537. (b) Schwemlein, H.; Brintzinger, H. H. *J. Organomet. Chem.* **1983**, *254*, 69–73.
(31) Sinnema, P.-J.; Shapiro, P. J.; Höhn, B.; Bitterwolf, T. E.; Twamley, B. *Organometallics* **2001**, *20*, 2883–2888.
(32) Tan, T.-S.; Fletcher, J. L.; McGlinchey, M. J. *J. Chem. Soc., Chem. Commun.* **1975**, 771–772.
(33) Eilbracht, P.; Henkes, E.; Totzauer, W.; Landers, A. *J. Chem. Soc., Chem. Commun.* **1980**, 717–718.
(34) Computational studies have previously shown the ferrocene unit to stabilize carbon-centered radical species via spin delocalization. For details see: Creary, X. *Org. Lett.* **2000**, *2*, 2069–2072.
(35) Hicks, R. G. *Org. Biomol. Chem.* **2007**, *5*, 1321–1338.
(36) Rinehart, K. L., Jr.; Frerichs, A. K.; Kittle, P. A.; Westman, L. F.; Gustafson, D. H.; Pruett, R. L.; McMahon, J. E. *J. Am. Chem. Soc.* **1960**, *82*, 4111–4112.
(37) Herbert, D. E.; Mayer, U. F. J.; Gilroy, J. B.; López-Gómez, M. J.; Lough, A. J.; Charmant, J. P. H.; Manners, I. *Chem.—Eur. J.* **2009**, *15*, 12234–12246.
(38) The first stable radical (Ph_3C•) was generated by C−C bond homolysis; for details, see: Gomberg, M. *J. Am. Chem. Soc.* **1900**, *22*, 757–771.

Scheme 4. Sodium-Mediated Reductive Coupling of 6,6-Dimethylfulvene and Its Application in the Synthesis of **1** [36]

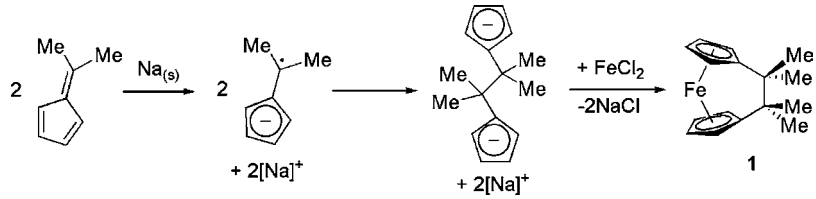

Scheme 5. Products from Cocondensation of 6,6-Dimethylfulvene with Iron Vapor[a]

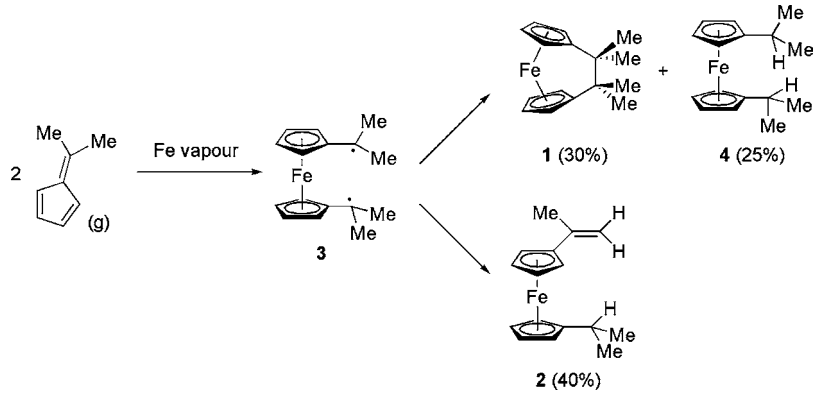

[a] **1** and **4**, as reported in ref 32, and **2**, as described in ref 33.

Scheme 6. Thermal Carbon−Carbon Bond Cleavage in *rac*-**5**

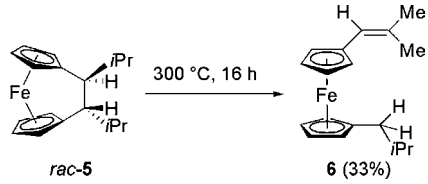

Scheme 7. Thermal Isomerization of *meso*/*rac*-**7**

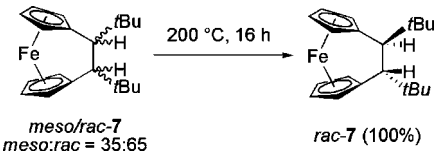

Notably, the C−C bond distance in the bridge is significantly shorter in the *rac* isomer [1.565(7) Å] compared with *meso*-**7** [1.612(3) Å]. Interestingly, the tilt angle of the two Cp rings is smaller for the *meso* isomer [$\alpha = 23.3(1)°$] than for the *rac* isomer [$\alpha = 25.5(2)°$]. This is surprising given that increasing the tilt angle between the two Cp rings of ferrocene has been calculated to raise the overall energy of the metallocene.[9,10] Steric repulsion between the *t*Bu substituents appears to lead to the longer C−C distance in the bridge of the *meso* isomer, which allows for a smaller tilt angle. As expected from the thermal isomerization, however, DFT calculations indicate that the optimized structure for *rac*-**7** is approximately 10 kcal mol^{-1} more stable than that of *meso*-**7** (*vide infra*).[39]

2.2. Further Insight into the Electronic Structure of Dicarba[2]ferrocenophanes 1, *rac*-5, and *rac*-7 Using UV–vis Spectroscopy and Cyclic Voltammetry. The three dicarba[2]ferrocenophanes, **1**, *rac*-**5**, and *rac*-**7** exhibit UV−vis absorption spectra consistent with their strained character (Figure 4).[11] The characteristic red shift of the lowest energy absorption band, λ_{max}, and increased molar absorptivity relative to ferrocene that accompanies tilting the Cp rings of [2]ferrocenophanes, is pronounced in **1**, *rac*-**5**, and *rac*-**7**. The position of this band reverts to higher energy and lower intensity in the ring-opened products **2** and **6** (Table 1). Alkyl substitution of the bridge carbons in **1**, *rac*-**5**, and *rac*-**7** induces a blue shift of λ_{max} compared with the $-CH_2CH_2-$ bridged 1,1'-ethylenyl[2]ferrocenophane ($\lambda_{max} = 476$ nm, $\varepsilon = 378$ M^{-1} cm^{-1}).[41] A similar trend was observed for a series of silicon-bridged [1]ferrocenophanes with varying degrees of methylation of the Cp rings.[20] This is most apparent in *rac*-**7** as the *t*Bu substituents exert the largest inductive effect on the [2]ferrocenophane moiety. Consistent with this, electrochemical studies revealed that due to the electron-rich *t*Bu substituents, *rac*-**7** is oxidized more easily than **1** or *rac*-**5** (Table 1).

For the ring-opened products, the substituents on the terminus of the alkene functionality appear to have the greatest influence on the oxidation potentials. The observed trends may be the result of conjugation of the ferrocene moiety with the alkene substituents, allowing for more effective electronic communication between the ferrocene and the electron-rich alkyl substituents. Accordingly, it is easier to oxidize compound **6** with two methyl groups distal to the Cp ring, compared with **2** which contains a methyl group adjacent to the Cp ring and two hydrogens at the distal end of the double bond. These groups lead to a more negative oxidation potential for **6** ($E_{1/2} = -0.10$ V) compared to compound **2** ($E_{1/2} = -0.03$ V), despite the second Cp ring in **2** containing the more inductively donating *i*Pr group compared with the isobutyl substituent of **6**. The CVs of **1** and **2** are shown in Figure 5, illustrating the shift of $E_{1/2}$ to a more positive potential in the ring-opened ferrocenes relative to the strained dicarba[2]ferrocenophane precursors.

(39) The energy penalty associated with an increase in tilt angle from 23.3(1)° to 25.5(2)° in ferrocene is *ca*. 5 kcal mol^{-1}. For details, see ref 9.

(40) Laing, M. B.; Trueblood, K. N. *Acta Crystallogr.* **1965**, *19*, 373–381.

(41) Barr, T. H.; Watts, W. E. *J. Organomet. Chem.* **1968**, *15*, 177–185.

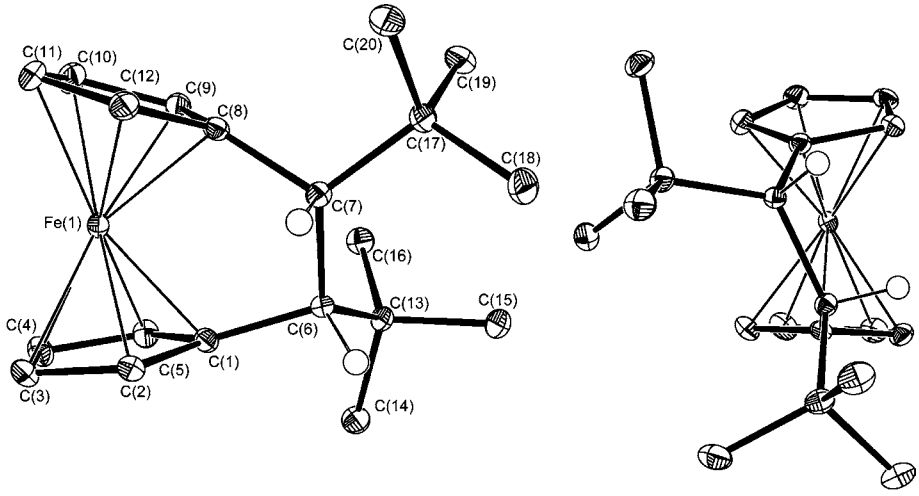

Figure 2. Solid-state structure of *meso*-**7**. Thermal ellipsoids shown at 50% probability levels. For clarity, only the hydrogens on the bridging carbons are shown. Selected bond lengths (Å) and angles (deg): C1−C6 = 1.539(3), C6−C7 = 1.612(3), C7−C8 = 1.541(3), C1−C6−C13 = 113.2(2), C8−C7−C17 = 112.7(2).

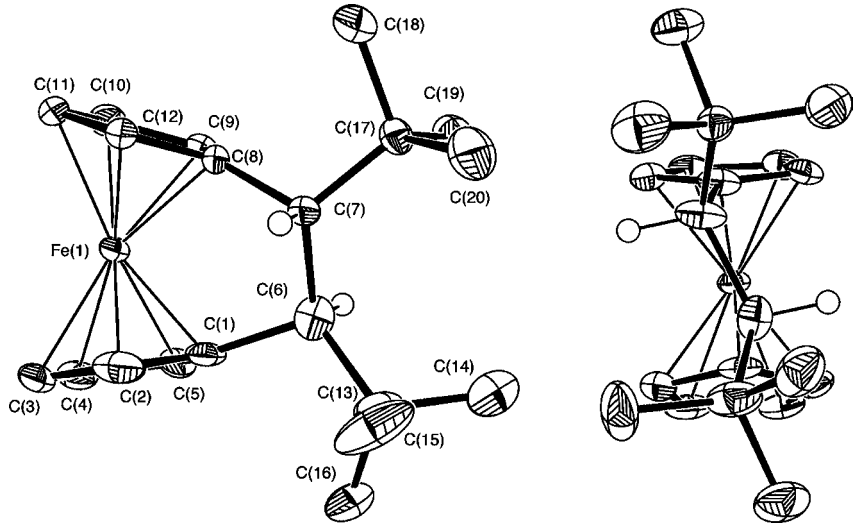

Figure 3. Solid-state structure of *rac*-**7**. Thermal ellipsoids shown at 50% probability levels. For clarity, only the hydrogens on the bridging carbons are shown. Selected bond lengths (Å) and angles (deg): C1−C6 = 1.542(7), C6−C7 = 1.565(7), C7−C8 = 1.577(7), C1−C6−C13 = 110.6(4), C8−C7−C17 = 109.5(4).

2.3. Attempted Trapping of Proposed Diradical Intermediates in Thermal Ring-Opening Reactions of Dicarba[2]ferrocenophanes 1, *rac*-5, and *rac*-7. As we hypothesized that the C−C bond cleavage observed in **1**, *rac*-**5**, and *rac*-**7** occurs via a homolytic C−C bond cleavage mechanism to afford a diradical intermediate, the thermal isomerization of *meso*-**7** to *rac*-**7** was repeated in the presence of potential radical traps 2,2,6,6-tetramethylpiperidine-1-oxyl (TEMPO) and butylated hydroxytoluene (BHT), a source of a stable phenoxyl radical. The *t*Bu substituents on the bridge of *meso*- and *rac*-**7** were expected to lend the most stability to the postulated diradical intermediates (*meso*- and *rac*-**8**, Scheme 8) due to the absence of hydrogen atoms α to the radical. However, in both trapping reactions, isomerization from *meso* to *rac* proceeded unhindered and increased amounts of *rac*-**7** were isolated from each reaction.[42] In the case of TEMPO, the trapping agent was observed to decompose at elevated temperatures (200 °C) over the course of the reaction. Unsuccessful trapping of the diradical intermediates is not inconsistent with the suggested mechanism. For example, it is possible that the electronic structure of the diradical involves a significant contribution from fulvene-based resonance forms (*meso*- and *rac*-**8**', Scheme 8), leading to lower

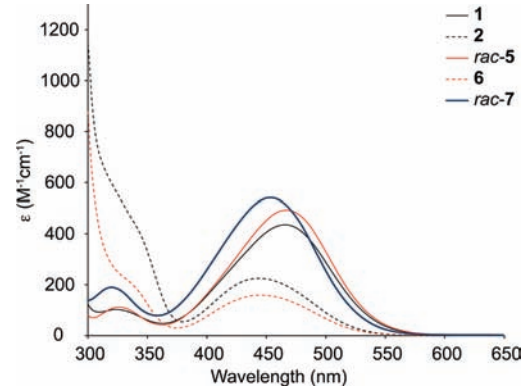

Figure 4. UV−vis spectra of **1**, **2**, *rac*-**5**, **6**, and *rac*-**7**.

(42) Variable temperature (25−250 °C) electron paramagnetic resonance (EPR) spectroscopy of *meso*/*rac*-**7** did not reveal the presence of observable paramagnetic species.

Table 1. Solution and Solid-State Characterization of Dicarba[2]metallocenophanes and Ring-Opened Metallocenes

M = Fe	**1**	**2**	*rac*-**5**	**6**	*meso*-**7**	*rac*-**7**
λ_{max} (nm), ε ($M^{-1}cm^{-1}$)[a]	466, 435	444, 225	466, 515[37]	447, 157	–	454, 540
$E_{1/2}$[b](V)	−0.06	−0.03	−0.06[37]	−0.10	–	−0.10
α (°)	23.2[40]	–	23.8 (1)[37]	–	23.3 (1)	25.5 (2)
Bridge C−C (Å)	1.584[40]	–	1.559 (3)[37]	–	1.612 (3)	1.565 (7)

M = Ru	**10**	**11**	*rac*-**12**	**14**	*meso*-**15**	*rac*-**15**
λ_{max} (nm), ε ($M^{-1}cm^{-1}$)[a]	351, 1225	317, 381	355, 2016	319, 623	–	346, 1731
α (°)	31.2 (3)[15]	–	31.0 (2)	–	30.2 (1)	33.6 (1)
Bridge C−C (Å)	1.599 (8)[15]	–	1.552 (5)	–	1.626 (2)	1.589 (9)

[a] In hexanes. [b] In CH_2Cl_2: referenced vs $Fe(C_5H_4)_2/Fe(C_5H_4)_2^+$.

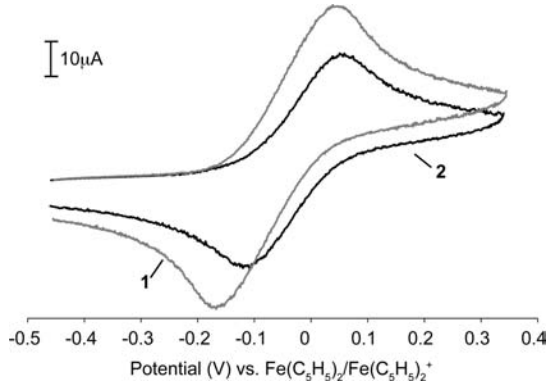

Figure 5. Cyclic voltammograms of CH_2Cl_2 solutions of **1** and **2** referenced to $Fe(C_5H_5)_2/Fe(C_5H_5)_2^+$ (scan rate = 200 mV s^{-1}; 0.1 M [nBu$_4$N][PF_6], 1 mM analyte).

Scheme 8. Possible Resonance Forms of the Intermediates Involved in the Isomerization of *meso*/*rac*-**7**

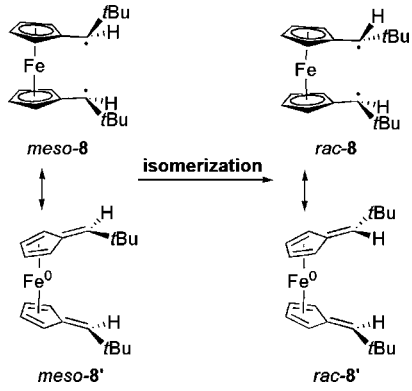

reactivity with radical traps. It is also possible that the bond resulting from the coupling of the trapping agents with the proposed radical intermediates is not stable at the elevated temperatures employed. An example of a bis(fulvene)iron complex (**9**), related to the postulated diradical intermediate through resonance, has been isolated at low temperature and crystallographically characterized (Scheme 9).[43]

2.4. Thermal Reactivity of Dicarba[2]ruthenocenophanes. To compare the reactivity of dicarba[2]ferrocenophanes with ruthenium-containing analogues, we synthesized a similar series of dicarba[2]ruthenocenophanes. These compounds were expected to possess greater degrees of ring strain than their iron counterparts as a result of the wider tilt angles forced onto the two Cp rings by the *ansa* bridge, due to the presence of a larger

(43) Teuber, R.; Köppe, R.; Linti, G.; Tacke, M. *J. Organomet. Chem.* **1997**, *545*−*546*, 105–110.

Scheme 9. Synthesis of Bis(diphenylfulvene)iron[43]

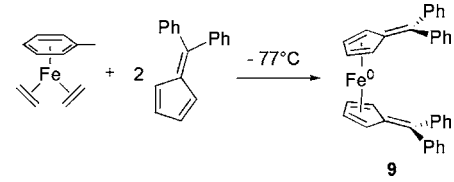

Scheme 10. Thermolysis of **10**

transition metal ion. For example, Ru−Cp bonds reduce their hapticity when dicarba[2]ruthenocenophanes react with diphosphines to produce ring-slipped products under ambient conditions, whereas analogous reactivity in less strained dicarba[2]ferrocenophanes requires photoactivation.[15] Furthermore, increased ring strain in dicarba[2]ruthenocenophanes has been illustrated in thermal ROP reactions, which occur at 220 °C for unsubstituted dicarba[2]ruthenocenophanes and at 300 °C for analogous dicarba[2]ferrocenophanes (Scheme 2).[26] The dicarba[2]ruthenocenophanes were prepared from the appropriate "fly-trap" ligands using the ligand stabilized metal precursor, *cis*-$RuCl_2(DMSO)_4$. The resulting dicarba[2]ruthenocenophanes were also found to undergo C−C bond cleavage at elevated temperatures to give ring-opened 1,1'-disubstituted ruthenocenes. Interestingly, while heating **1** to 240 °C for 1.5 h led to 39% conversion to the ring-opened **2**, similar treatment of 1,1'-tetramethylethylenyl[2]ruthenocenophane **10** [melting point = 129 °C; α = 31.2(3)°; cf. **1** α = 23.2°] afforded the intramolecular H• abstraction product **11** quantitatively (Scheme 10).

The dicarba[2]ruthenocenophane analogue of *rac*-**5** was similarly prepared and fully characterized (melting point = 224 °C). Pure *rac*-**12** was isolated by sublimation and recrystallization and fully characterized. The high tilt angle [α = 31.0(2)°, Figure 6] between the two Cp rings of *rac*-**12** indicated a high degree of ring strain comparable to that of **10** [α = 31.2(3)°]. Heating *rac*-**12** for 1.5 h at 300 °C, however, did not result in any observable conversion to the ring-opened product **14**. Instead, ^{1}H NMR spectroscopic analysis of the mixture obtained following heating *rac*-**12** at 300 °C for 16 h showed only 66% conversion to **14**. The disproportionation of *rac*-**12** to **14** is a slow reaction; however, higher conversion is observed for the thermal ring opening of *rac*-**12** compared to the analogous iron complex *rac*-**5** (33% conversion to **6** under

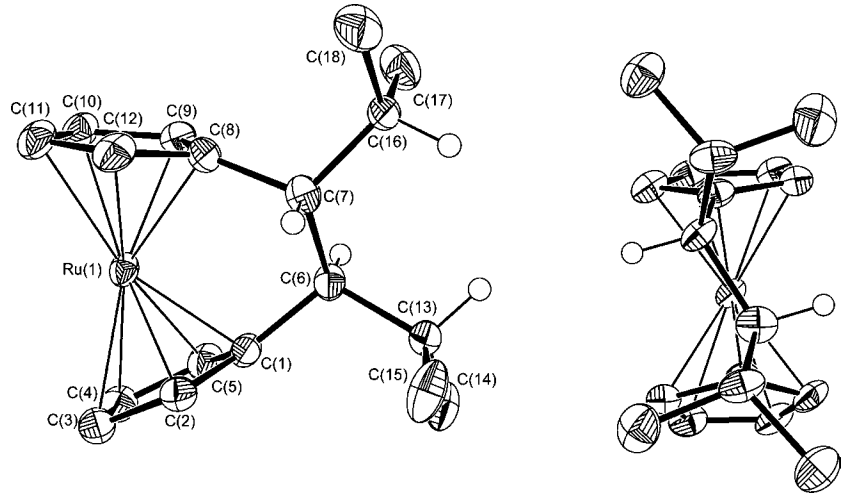

Figure 6. Solid-state structure of *rac*-**12**. Thermal ellipsoids shown at 50% probability levels. For clarity, only *i*Pr and bridging hydrogens on the bridging carbons are shown. Selected bond lengths (Å) and angles (deg): C1−C6 = 1.530(7), C6−C7 = 1.553(8), C7−C8 = 1.542(8), C1−C6−C13 = 111.4(4), C8−C7−C16 = 113.2(5).

Scheme 11. Thermolysis of *rac*-**12**

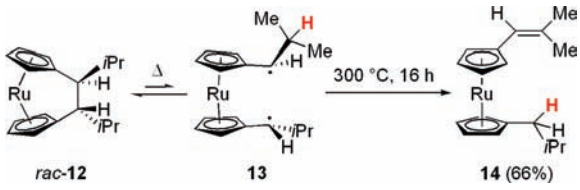

Scheme 12. Thermal Isomerization of *meso*/*rac*-**15**

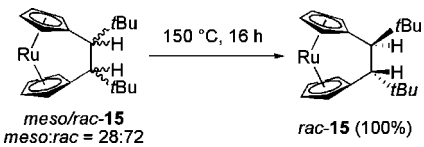

similar conditions). This suggests that the greater ring strain of *rac*-**12** compared to *rac*-**5** allows for C−C bond cleavage to occur more easily, driving the equilibrium toward the postulated diradical intermediate **13**, which may undergo intramolecular H• abstraction to produce **14** (Scheme 11). The observed reactivity trends confirm that the C−C bond cleavage in tetramethyl-substituted dicarba[2]metallocenophanes occurs more readily than isopropyl substituted dicarba[2]metallocenophanes and that the introduction of a larger transition metal, i.e., ruthenium, allows for C−C bond cleavage to occur more easily compared to analogous iron containing compounds.

A mixture of *meso*- and *rac*-1,1'-di-*tert*-butylethylenyl-[2]ruthenocenophane (*meso*/*rac*-**15**) was prepared in a similar manner to the iron derivative *meso*/*rac*-**7** and fully characterized (melting point of the mixture = 120−125 °C). An isomeric ratio of 28:72 (*meso*:*rac*) was determined from ^{1}H NMR spectroscopy of the as-prepared sample, and this sample was employed in further reactivity studies. The thermal isomerization of *meso*-**15** to *rac*-**15** also proceeded in the melt. A sample of *meso*/*rac*-**15** was sealed in a glass tube and heated for 16 h at 150 °C (Scheme 12). After heating, quantitative conversion to pure *rac*-**15** was detected by ^{1}H NMR spectroscopy and the pure product (melting point = 155 °C) was isolated, allowing for its comprehensive characterization. As expected from a comparison of the tilt angles of *meso*-**7** [α = 23.3(1)°] and *meso*-**15** [α = 30.2(1)°, Figure 7], the isomerization of the more strained dicarba[2]ruthenocenophane is more facile and occurs quantitatively at a lower temperature. After the reaction temperature was lowered closer to the melting point of the mixture of *meso*/*rac*-**15** (135 °C) followed by heating for 16 h, the sample was at first mobile but had visibly solidified after 16 h. The starting material was recovered in 93% yield and the ratio of isomers only changed slightly in favor of *rac*-**15** to 17:83 (*meso*:*rac*).

Interestingly, as was observed in the crystal structures of *meso*- and *rac*-**7**, the tilt angle of the two Cp rings in *meso*-**15** [α = 30.2(1)°, Figure 7] is smaller than that of *rac*-**15** [α = 33.6(1)°, Figure 8]. Accordingly, the bridging C−C bond in *rac*-**15** is shorter [1.596(9) Å] than that in the less stable *meso*-**15** [1.626(2) Å]. As for the [2]ferrocenophanes, reducing the length of the bridging C−C bond between the *t*Bu substituents results in slightly higher α angles for the *rac* isomer. The moderate difference in C−C bond distance within the [2]ferrocenophanes (ΔC−C = 0.047(8) Å) compared to the analogous [2]ruthenocenophanes (ΔC−C = 0.037(9) Å) may reflect the reluctance of the Cp rings of *meso*- and *rac*-**15** to increase the already substantial tilt angle associated with the larger transition metal ion.[44]

The bridging C−C bonds of the [2]metallocenophanes discussed in this work might be compared to the C−C bridges of [2.2]paracyclophane, a strained molecule known to undergo thermal polymerization to generate poly(phenylene vinylene).[45] ROP in this case is proposed to proceed by thermal cleavage of bridging C−C bonds to form 2 equiv of a reactive intermediate, *p*-xylylene, which then polymerizes (Scheme 13).[46] At 1.580(1) Å,[47] the bridging C−C bonds in [2.2]paracyclophane fall within the range of the bridging C−C bond lengths in our series of dicarba[2]metallocenophanes (Table 1: 1.552(5)−1.626(2) Å). The bridging C−C bonds in *meso*-**7** and *meso*-**15** are the longest of the series [1.612(3) and 1.626(2) Å, respectively], suggesting these bonds are the most weakened. The longer C−C bond in the dicarba[2]ruthenocenophane *meso*-

(44) The relative energy penalty associated with changes in tilt-angle in ferrocenes has previously been shown to increase as the relevant tilt angles increase; i.e., the slope of the energy vs tilt angle plot increases at higher tilt angle. For details, see ref 9.
(45) (a) Iwatsuki, S. *Adv. Polym. Sci.* **1984**, *58*, 93–120. (b) Iwatsuki, S.; Kubo, M.; Yamashita, H. *Chem. Lett.* **1989**, 729–732.
(46) Szwarc, M. *Nature* **1947**, *160*, 403.
(47) Lyssenko, K. A.; Antipin, M. Y.; Antonov, D. Y. *ChemPhysChem* **2003**, *4*, 817–823.

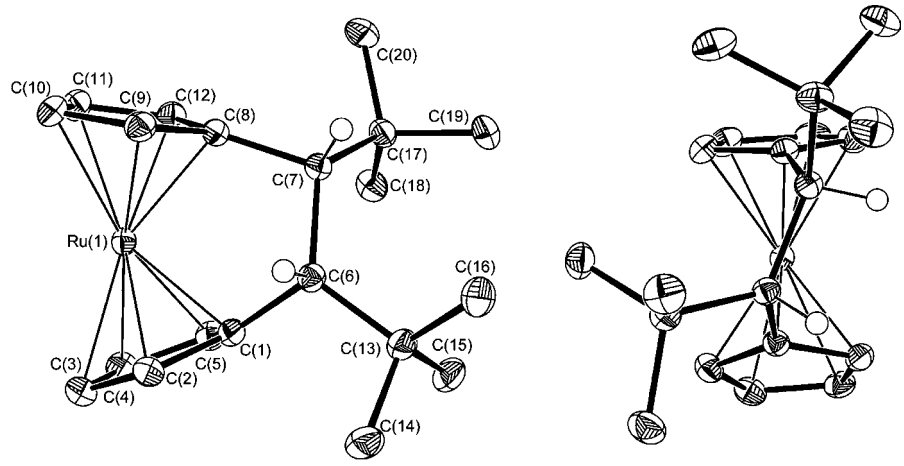

Figure 7. Solid-state structure of *meso*-**15**. Thermal ellipsoids shown at 50% probability levels. For clarity, only the hydrogens on the bridging carbons are shown. Selected bond lengths (Å) and angles (deg): C1−C6 = 1.553(2), C6−C7 = 1.626(2), C7−C8 = 1.556(2), C1−C6−C13 = 111.6(1), C8−C7−C17 = 112.3(1).

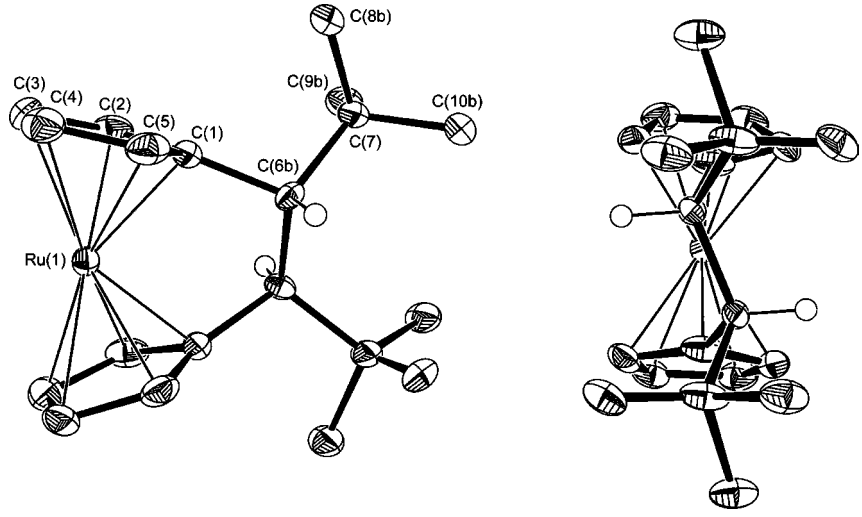

Figure 8. Solid-state structure of *rac*-**15**. Thermal ellipsoids shown at 50% probability levels. For clarity, only the hydrogens on the bridging carbons are shown. Selected bond lengths (Å) and angles (deg): C1−C6$_b$ = 1.596(6), C6$_a$−C6$_b$ = 1.589(9), C1−C6$_b$−C7 = 105.9(3).

Scheme 13. Thermal ROP of [2.2]Paracyclophane

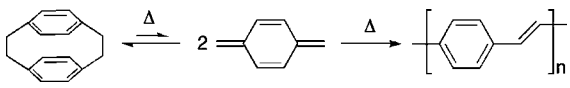

15 is consistent with a larger α angle compared with the iron congener *meso*-**7**, as a shorter C−C bond would require a further increase in the already substantial tilt of the two Cp rings. The difference in energy between the two dicarba[2]ruthenocenophane isomers was also examined by DFT calculations, with *rac*-**15** calculated to lie ∼10 kcal mol^{-1} in energy lower than *meso*-**15**, similar to what was found for dicarba[2]ferrocenophanes *meso*/*rac*-**7** (*vide infra*).

2.5. Computational Studies of the Isomerization of *meso*-7 and *meso*-15. To further probe the mechanism of C−C bond cleavage in dicarba[2]metallocenophanes, DFT calculations using the B3PW91 functional and DZP quality basis sets were employed. The *meso* to *rac* isomerization of *meso*/*rac*-**7** and *meso*/*rac*-**15** was studied exclusively, as computational studies of the C−C bond cleavage in other derivatives may be complicated by the reactivity of the intermediates (i.e., disproportionation reactions). We propose a homolytic bond cleavage mechanism (Scheme 14), corroborated by the reactivity trends observed, and the synthetic pathways used to form the C−C bond in ligand precursors (see Scheme 4).

The ferrocenophane *meso*-**7** and ruthenocenophane *meso*-**15** were found to be higher in energy than the *rac*-isomers, likely due to steric interactions between bulky *t*Bu groups (Table 2). Homolytic C−C bond cleavage may occur, presumably without a barrier above the endothermicity of the overall reaction, to give the corresponding diradical species. For convenience, all diradical species were treated as open shell triplets (*vide infra*). A number of conformers are possible as the Cp rings can rotate about the Cp−M−Cp bond axis and the substitutents on the two Cp rings can also rotate with respect to each other. In this study, we report the energies for the lowest-lying conformers that we located, only considering cases where the two substituents remain fairly close. More extensive rotation around the Cp−M−Cp axis, which may lead to very slightly lower energies, was not considered here (Table 2). From these radical intermediates, transition states *ts*-**8** (*M* = Fe) or *ts*-**16** (*M* = Ru) can be accessed, where bond rotation occurs around a C_{ipso}−C*t*Bu bond, and the hydrogen atom (shown in red, Scheme 14) displays the highest displacement vector with respect to other parts of the molecule. The transition state and

Scheme 14. Homolytic C−C Bond Cleavage Leading to Isomerization of *meso*-**7** and *meso*-**15**

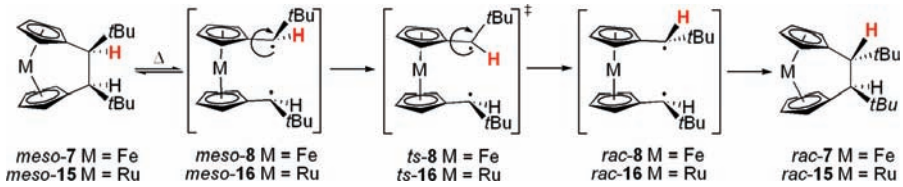

Table 2. Relative Energies of Potential Intermediates in the *meso* to *rac* Isomerization of *meso*/*rac*-**7** and *meso*/*rac*-**15** (kcal mol^{-1})

M = Fe	ΔE^a	ΔH^b	ΔG^c	M = Ru	ΔE^a	ΔH^b	ΔG^c
rac-**7**	0	0	0	*rac*-**15**	0	0	0
rac-**8**	27.4	29.0	23.5	*rac*-**16**	21.9	23.4	17.8
ts-**8**	37.8	39.2	33.2	*ts*-**16**	29.9	31.0	25.4
meso-**8**	27.9	29.5	23.5	*meso*-**16**	22.7	24.1	18.2
meso-**7**	10.1	10.0	10.8	*meso*-**15**	9.3	9.1	9.8
rac-**17**	36.8	38.0	34.5	*rac*-**18**	17.9	19.0	15.4
meso-**17**	38.2	39.3	36.0	*meso*-**18**	19.1	20.0	16.8

[a] ΔE = Potential energy with zero-point correction. [b] ΔH = enthalpy at 298 K. [c] ΔG = Gibb's free energy at 298 K.

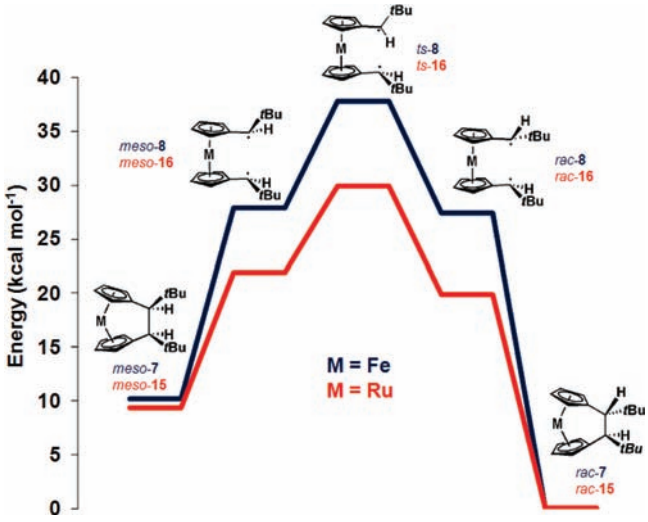

Figure 9. Proposed reaction pathway for the *meso* to *rac* conversion of *meso*/*rac*-**7** and *meso*/*rac*-**15**.

the radical intermediates are higher in energy for the Fe case than for Ru (Table 2 and Figure 9), which is consistent with the reactivity trends discussed above, where increased ring strain in dicarba[2]ruthenocenophanes relative to dicarba[2]ferrocenophanes allowed C−C cleavage reactions to proceed further toward completion or isomerization to occur at lower temperatures.

The formation of diradical intermediates in the *meso* to *rac* isomerization of *meso*/*rac*-**7** and *meso*/*rac*-**15** may be relevant to the mechanism of thermal ROP in $-CH_2CH_2-$ bridged dicarba[2]metallocenophanes as both sets of compounds lack hydrogen atoms α to the proposed radical. As discussed previously, the α-hydrogen atoms in other derivatives may be involved in intramolecular disproportionation reactions. For *meso*- and *rac*-**7** and **15**, the steric interactions of *t*Bu substitutents would be expected to favor intramolecular C−C bond formation to regenerate the cyclic precursor, while an unsubstituted ($-CH_2CH_2-$) backbone in other derivatives may allow for polymerization to occur via intermolecular coupling of CH_2 centered radicals to generate a linear polymetallocene (Scheme 15).

To further understand the reactivity observed upon C−C bond cleavage in dicarba[2]metallocenophanes, the optimized structures of diradicals *meso*- and *rac*-**8** and **16** were inspected. The

Scheme 15. Proposed Mechanism for the Thermal Polymerization of Dicarba[2]metallocenophanes

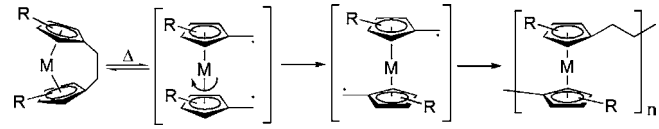

bond lengths between the *ipso*-carbons and the *C*H*t*Bu groups for the triplet intermediates were 1.405 and 1.405 Å (*rac*-**8**), 1.403 and 1.405 Å (*meso*-**8**), 1.422 and 1.422 Å (*rac*-**16**), and 1.420 and 1.422 Å (*meso*-**16**), which fall between typical C−C (1.53 Å) and C=C bonds (1.34 Å).[48] We interpret this as evidence that the C_{ipso}−CH*t*Bu bond has some double bond character in the postulated diradical intermediates, implying partial bis(fulvene)metal(0) character as discussed previously (Scheme 8). Furthermore, the sum of the bond angles about the CH*t*Bu carbon was 360° for each of the optimized structures, corroborating a planar sp^2 environment. Inspection of the overall spin density in *rac*-**8** reveals this to reside primarily on the *C*H*t*Bu carbon atoms, which suggests the open shell intermediate also has signficant diradical character (Figure 10). The apparent diradical characteristics are consistent with a thermally induced H• abstraction pathway for **1**, *rac*-**5**, **10**, and *rac*-**12**, as well as the thermally induced pathway proposed for the isomerization of *meso*- to *rac*-**7** and **15**.

The bulk of our calculations addressed only the triplet form of the intermediates and isomerization transition states. This was due to computational convenience, as noted above, because singlet calculations proved difficult to converge in some cases. Also, the presence of metal centers would probably enable a mechanism involving double spin-state change through a triplet intermediate.[49] However, isomerization should be able to occur purely on the singlet surface. In the absence of strong mixing of the diradical (*meso*- and *rac*-**8**) and bis(fulvene) (*meso*- and *rac*-**8'**) resonance forms, the singlet surfaces should follow the triplet surfaces quite closely, and the trends derived from the triplet calculations described above should be qualitatively correct.

(48) *CRC Handbook of Chemistry and Physics*, 89th ed.; Lide, D. R., Ed.; CRC Press: Boca Raton, FL, 2009.
(49) For reviews on such spin-forbidden processes, see: (a) Poli, R.; Harvey, J. N. *Chem. Soc. Rev.* **2003**, *32*, 1–8. (b) Besora, M.; Carreón-Macedo, J.-L.; Cimas, Á.; Harvey, J. N. *Adv. Inorg. Chem.* **2009**, *61*, 573–623.

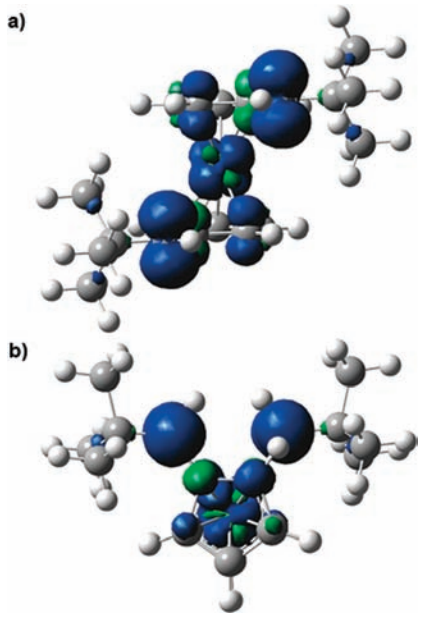

Figure 10. Spin density plot for *rac*-**8**: (a) side view and (b) top view (iso value = 0.005).

Nevertheless, interesting additional bonding options are possible on the singlet potential energy surface, and limited additional calculations were therefore carried out to investigate their potential role. Singlet species related to the bis(fulvene) resonance forms *meso*- and *rac*-**8**' can be described using a conventional closed-shell ansatz, whereas the singlet state of the diradical resonance forms *meso*- and *rac*-**8** requires an unrestricted method. Single-point energy calculations at the optimized geometry of the triplet transition states *ts*-**8** and *ts*-**16** using an unrestricted approach yielded energies 0.4 kcal mol^{-1} (Fe) and 6.2 kcal mol^{-1} (Ru) higher than the triplet energies. However, geometry convergence for this type of calculation proved difficult, and these studies were therefore not pursued further. Closed-shell singlet calculations for the intermediates *meso*- and *rac*-**8** and **16** provide insight into the possible role of complexes bearing fulvene-like ligands. Considerable distortion occurs upon geometry optimization, leading to the new species *meso*- and *rac*-**17** and **18**, respectively, for Fe and Ru. These structures, which are related to both diradical and bis(fulvene) structures through resonance, involve one CpCH*t*Bu fragment bound via an η^5-Cp ligand and the CH*t*Bu carbon atom.[50] The second ligand is bound in an η^4 fashion and appears to have significant fulvene character. The formation of M−C bonds of this type in 'tuck-in' metallocenes is relatively rare, however, several structurally characterized examples incorporating a variety of transition metals have been reported.[51]

In the case of *meso*- and *rac*-**17**, the optimized structures lie much higher in energy than the triplet diradical and presumably do not intervene significantly in the reactivity. For Ru, however, the energies are close, and the intermediates may have significant

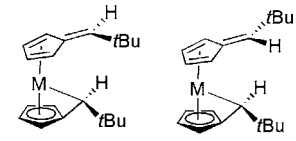

meso-**17** M = Fe *rac*-**17** M = Fe
meso-**18** M = Ru *rac*-**18** M = Ru

fulvene character at one of the Cp-based ligands. It is to be noted, however, that rotation around the C_{ipso}−CH*t*Bu bond in such structures should highly destabilize the bis(fulvene) form, so that, even with Ru, the rate-limiting transition state for the *meso* to *rac* isomerization is probably similar to the diradical *ts*-**16** discussed above.[52]

3. Summary

Heating the strained, dicarba[2]ferrocenophanes **1**, *rac*-**5**, and *meso*/*rac*-**7** in the melt led to slow cleavage of the C−C bond in the bridge, in analogy to the ROP of [2.2]paracyclophanes. However, instead of undergoing polymerization, intramolecular abstraction of H• from one substituent yielded ring-opened, vinyl-substituted 1,1'-metallocenes from **1** and *rac*-**5**, while, in the case of the *t*Bu substituted *meso*/*rac*-**7**, the bulky, strongly donating substituents stabilized the likely diradical intermediates (*meso*- and *rac*-**8**), and *meso*-**7** thermally converted to the more stable *rac* isomer. The corresponding dicarba[2]ruthenocenophanes underwent thermal C−C bond cleavage more readily, consistent with a higher degree of ring strain. Despite exhibiting a higher tilt angle (α/deg) between the two Cp rings, calculations showed the *rac* isomer in each case to be more stable by ∼10 kcal mol^{-1}. Computational studies support the proposed homolytic C−C bond cleavage mechanism and indicate that the intermediates may also have some fulvene character, providing insight into the isomerization pathway between *meso*- and *rac*-*t*Bu substituted dicarba[2]metallocenophanes as well as the intramolecular H• abstraction reactions observed in other derivatives. This study also led to insight into the likely mechanism of the thermal polymerization of $-CH_2CH_2-$ bridged dicarba[2]metallocenophanes[25−27] and for the first time provides support for a homolytic C−C bond cleavage pathway.[53]

Future work involving the stabilization of relevant diradical intermediates generated by thermolysis of strained dicarba[2]-metallocenophanes may provide an entry point to unique, disubstituted *ansa*-metallocenes and multimetallic complexes, and the investigation of several new areas of dicarba[2]metallocenophane chemistry is ongoing in our lab. Our current pursuits

(50) This arrangement is analogous to that previously noted in the bis(silyl) molybdenocene 'tuck-in' product of Scheme 2 (ref 24). Interactions resembling the M−CH*t*Bu interactions have also been observed in ferrocenylboranes and ferrocene-stabilized carbocations. For details, see: (a) Scheibitz, M.; Bolte, M.; Bats, J. W.; Lerner, H.-W.; Nowik, I.; Herber, R. H.; Krapp, A.; Lein, M.; Holthausen, M. C.; Wagner, M. *Chem.*−*Eur. J.* **2005**, *11*, 584–603. (b) Kreindlin, A. Z.; Dolgushin, F. M.; Yanovsky, A. I.; Kerzina, Z. A.; Petrovskii, P. V.; Rybinskaya, M. I. *J. Organomet. Chem.* **2000**, *616*, 106–111.

(51) (a) Cloke, F. G. N.; Green, J. C.; Green, M. L. H.; Morley, C. P. *J. Chem. Soc., Chem. Commun.* **1985**, 945–946. (b) Bulls, A. R.; Schaefer, W. P.; Serfas, M.; Bercaw, J. E. *Organometallics* **1987**, *6*, 1219–1226. (c) Schock, L. E.; Brock, C. P.; Marks, T. J. *Organometallics* **1987**, *6*, 232–241. (d) Rybinskaya, M. I.; Kreindlin, A. Z.; Struchkov, Y. T.; Yanovsky, A. I. *J. Organomet. Chem.* **1989**, *359*, 233–243. (e) Fischer, J. M.; Piers, W. E.; Young, V. G., Jr. *Organometallics* **1996**, *15*, 2410–2412. (f) Evans, W. J.; Miller, K. A.; DiPasquale, A. G.; Rheingold, A. L.; Stewart, T. J.; Bau, R. *Angew. Chem., Int. Ed.* **2008**, *47*, 5075–5078. (g) Zachmanoglou, C. E.; Lee, H.; Jang, S. H.; Pang, K.; Parkin, G. *Proc. Natl. Acad. Sci. U.S.A.* **2008**, *105*, 11060–11065.

(52) We have also explored the relationship between *meso*-**18** and bis(fulvene)ruthenium structures. See Supporting Information for details.

(53) The proposed mechanism is further supported by the observation that $-CH_2CH_2-$ bridged [2]ferrocenophanes undergo thermal ROP while −CH=CH− bridged [2]ferrocenophanes do not. For details, see: Masson, G.; Lough, A. J.; Manners, I. *Macromolecules* **2008**, *41*, 539–547.

include the solution phase C−C bond cleavage and metal insertion chemistry of dicarba[2]metallocenophanes as well as mechanistic studies of the thermal ROP of other dicarba[2]metallocenophanes.

Acknowledgment. We thank the European Union for a Marie Curie Chair (I.M.), the Royal Society for a Wolfson Research Merit Award (I.M.), NSERC of Canada for a postgraduate scholarship (D.E.H.) and a postdoctoral fellowship (J.B.G.), and EPSRC (A.S.) for funding. We also thank Prof. Robin Perutz for helpful discussions and suggestions, Prof. Neil G. Connelly for the use of electrochemical equipment, and Dr. Christopher J. Adams for assistance with EPR measurements.

Supporting Information Available: Experimental, crystallographic, and computational details. This material is available free of charge via the Internet at http://pubs.acs.org.

JA9087049